

# FINITE-STATE WAKE INFLOW MODELS FOR ROTORCRAFT FLIGHT DYNAMICS IN GROUND EFFECT

Felice Cardito, Jacopo Serafini, Claudio Pasquali, Giovanni Bernardini, Massimo Gennaretti  
Roma Tre University, Department of Engineering  
Rome, Italy

Roberto Celi  
University of Maryland,  
College Park, USA

## Abstract

Rotor wake inflow plays a crucial role in rotorcraft aeromechanics and, on the other side, it is strictly dependent on the operating condition. The presence of the ground below the rotor disc affects rotor aerodynamics, especially through the modification of wake inflow with respect to free-air operative condition. Here, the effect of ground on wake inflow and aeromechanic response and stability is investigated. Linear, time-invariant dynamic inflow models, extracted from high-fidelity aerodynamic simulations and suited for aeromechanic analysis, are presented. One provides the wake inflow as a function of rotor kinematic variables, while the second one gives the wake inflow as forced by rotor loads. In both cases, first the involved transfer functions are identified through time-marching aerodynamic simulations, and then a rational-matrix formula is applied for their finite-state approximation. In-ground-effect and out-of-ground-effect state-space inflow models are applied for helicopter response and stability analyses, and the corresponding results are compared to discuss the influence of ground on aeromechanics.

## 1 INTRODUCTION

Near-ground helicopter operation modeling is a very challenging task. The flow around the helicopter is indeed made more complex by the interaction between the terrain and wake vortices. Moreover, from a piloting point of view, in-ground-effect flight procedures are much more difficult and dangerous due to a combination of factors: i) the reduced margin of maneuver; ii) the possible presence of gusts and wind shear; iii) the complexity of the tasks to be fulfilled. Note that, helicopter capability to hovering makes near-ground operations not limited to landing and take off, but also includes other tasks, like rescue operations.

Particularly severe threats to flight safety arise in landing over a ship moving deck<sup>[1]</sup>. This is due to several additional factors including the relatively small size of the flight deck, turbulence due to the wake released by ship or platform superstructures, and deck roll, pitch and heave motion induced by waves<sup>[2;3;4;5;6;7]</sup>. Thus, the ship deck effects on landing helicopter dynamics may be divided into two main categories: those deriving from the impingement of turbulent flow generated by the ship superstructure during motion, and those deriving from the presence of the deck below the vehicle that alters the rotor wake dynamics (ground effect). On first approximation, ship's airwake turbulence and helicopter rotor downwash effects may be superimposed (thus neglecting coupling phenomena). The estimation of the ship turbulent airwake effect on the helicopter dynamics

could be accomplished either through a control equivalent turbulence input approach, when suited experimental flight data are available<sup>[8]</sup>, or taking advantage of dedicated numerical simulations of the flow-field of ship's airwake shed from the superstructure<sup>[9;10;11]</sup>.

On the other hand, the effect of ground presence on rotor/helicopter aerodynamics (of common importance to any near-ground operation), has been studied by several authors in the past decades, starting with the pioneering experimental work of Wiesner and Kohler<sup>[12]</sup>, Yeager, Young and Mantay<sup>[13]</sup> and that of Empey and Ormiston<sup>[14]</sup>, that was followed by the studies presented by Curtiss et al.<sup>[15]</sup>, Hanker and Smith<sup>[16]</sup>, Cimbala et al.<sup>[17]</sup> and Light<sup>[18]</sup>.

More recently, this problem has been examined also through dedicated numerical models<sup>[19;20]</sup>. Among these, the adaptation of the well-known Peters and He's dynamic inflow model including the effect of a surface below the rotor has been proposed<sup>[21;22;23]</sup>. It is of particular interest for the rotorcraft manufacturer/research community in that, due to its simplicity and reduced computational effort, the use of dynamic inflow models coupled with two-dimensional airfoil aerodynamics still remains a widely-used approach. Despite the aforementioned advantages, this modelling suffers from the accuracy limitations of analytical or semi-analytical models, that may be particularly critical when dealing with complex interaction phenomena or non-conventional operating conditions.

Here, the authors present in-ground-effect helicopter

aeromechanics analysis through application of the rotor dynamic inflow model recently introduced by Gennaretti et al.<sup>[24]</sup>. It is derived from high-fidelity numerical aerodynamic predictions as an extension of the out-of-ground-effect wake inflow model introduced in the recent past<sup>[25;26;27;28]</sup>. The modeling technique is completely general and is applicable to ground of arbitrary shape and in arbitrary motion.

In the following, first the proposed wake inflow modelling technique is outlined, then the application to aeromechanics analysis is described, and finally results of a numerical investigation concerning a rotor hovering in proximity of the ground are discussed.

## 2 METHODOLOGY

In this section, the whole modeling scheme is presented. First, the dynamic inflow model identification procedure is illustrated, then the aerodynamic solver used for the inflow simulations and the aeromechanics tool are described.

### 2.1 Dynamic inflow modeling

Two different finite-state, In-Ground-Effect inflow models are here introduced and tested. The former, denoted as  $\lambda - q$ , relates wake inflow with controls and flight dynamics kinematic degrees of freedom (namely blade pitch controls, hub motion and rigid blade flapping variables), whereas the latter,  $\lambda - f$ , relates inflow with rotor thrust, roll and pitching moment coefficients  $\{C_T, C_L, C_M\}$ , similarly to the Pitt and Peters' model<sup>[29;30]</sup>.

The approximated expression of the wake inflow distribution over the rotor disc,  $\lambda_{app}$ , is expressed by the widely used linear interpolation formula, defined in a non-rotating polar coordinate system,  $(r_c, \psi)$ .

$$(1) \quad \lambda_{app}(r_c, \psi, t) = \lambda_0(t) + r_c (\lambda_s(t) \sin \psi + \lambda_c(t) \cos \psi)$$

where  $r_c$  denotes distance from the disc center,  $\psi$  is the azimuth angular distance from the rear blade position, and the coefficients,  $\lambda_0$ ,  $\lambda_s$  and  $\lambda_c$  represent, respectively, instantaneous mean value, side-to-side gradient and fore-to-aft gradient.

For the  $\lambda - q$  model, once the wake inflow over the blades corresponding to chirp-type perturbations about the steady state rotor kinematics variables (namely, hub motion components, blade flapping components, and blade pitch controls) is determined by the high fidelity aerodynamic solver, input and output signals are windowed and transformed into frequency domain in order to determine the sampled transfer matrix  $\mathbf{H}(\omega)$  such that

$$(2) \quad \tilde{\lambda} = \mathbf{H}\tilde{\mathbf{q}}$$

where  $\lambda = \{\lambda_0 \lambda_s \lambda_c\}^T$  and  $\mathbf{q} = \{q_v \ q_\Omega \ q_\beta \ q_\theta\}^T$ , with  $\mathbf{q}_v = \{u \ v \ w\}^T$  and  $\mathbf{q}_\Omega = \{p \ q \ r\}^T$  collecting, respectively, the hub linear and angular velocities,  $\mathbf{q}_\beta = \{\beta_0 \ \beta_s \ \beta_c\}^T$  the

blade flap components, and  $\mathbf{q}_\theta = \{\theta_0 \ \theta_s \ \theta_c\}^T$  the blade pitch controls.

Then, performing a rational-matrix approximation of  $\mathbf{H}$ <sup>[31;27]</sup>, and transforming into time domain provides the following state-space model

$$(3) \quad \begin{aligned} \dot{\lambda} &= \mathbf{A}_1 \dot{\mathbf{q}} + \mathbf{A}_0 \mathbf{q} + \mathbf{C} \mathbf{x} \\ \dot{\mathbf{x}} &= \mathbf{A} \mathbf{x} + \mathbf{B} \mathbf{q} \end{aligned}$$

where  $\mathbf{x}$  is the vector of the additional states representing the wake dynamics effects, whereas matrices  $\mathbf{A}_1, \mathbf{A}_0, \mathbf{A}, \mathbf{B}, \mathbf{C}$  are real, fully populated matrices derived from the rational-matrix approximation process.

Starting from the approach proposed above, an alternative procedure providing a dynamic inflow model relating the wake inflow coefficients,  $\lambda$ , to rotor loads perturbations (akin to the well-known Pitt-Peters model) can be developed. It requires the additional identification of the transfer function matrix  $\mathbf{G}$  between the kinematic input variables perturbations and the corresponding rotor loads,  $\mathbf{f}$ <sup>[25]</sup>.

Considering, for instance, blade control pitch perturbations,  $\mathbf{q}_\theta$ , and thrust, roll and pitch moments,  $\mathbf{f} = \{C_T, C_L, C_M\}^T$ , once the relations  $\tilde{\lambda} = \mathbf{H}(\omega) \tilde{\mathbf{q}}_\theta$  and  $\tilde{\mathbf{f}} = \mathbf{G}(\omega) \tilde{\mathbf{q}}_\theta$  are identified for each sampling frequency, the wake inflow coefficients are directly related to the rotor loads as

$$(4) \quad \tilde{\lambda} = \mathbf{H}\mathbf{G}^{-1}\tilde{\mathbf{f}}$$

Then, the rational approximation of the resulting transfer matrix followed by the transformation into time domain yields the following state-space representation of the inflow

$$(5) \quad \begin{aligned} \dot{\lambda} &= \hat{\mathbf{C}} \mathbf{x} \\ \dot{\mathbf{x}} &= \hat{\mathbf{A}} \mathbf{x} + \hat{\mathbf{B}} \mathbf{f} \end{aligned}$$

similar to that in Eq. (3), but given in terms of rotor loads<sup>[25]</sup>, and with the polynomial part removed due to the asymptotic behavior of  $\mathbf{G}$ .

Equivalent (but different) inflow models can be obtained starting from each triplet of kinematic DOFs considered in  $\lambda - q$  model.

### 2.2 Aerodynamic Solver

The Boundary Element Method solver<sup>[32;33]</sup> here used for wake inflow prediction, is suited for rotors in arbitrary motion and is capable of accurate simulations taking into account free-wake and aerodynamic interference effects in multi-body configurations, as well as severe body-vortex interactions; a finite ground below the rotor is modeled as an additional body<sup>[24]</sup>.

Considering incompressible, potential flows such that  $\vec{v} = \nabla\phi$ , the aerodynamics formulation applied assumes the potential field,  $\phi$ , given by the superposition of an incident field,  $\phi_I$ , and a scattered field,  $\phi_S$  (i.e.  $\phi = \phi_I + \phi_S$ ). The scattered potential is determined by sources and doublets distributions over the surfaces of the bodies,  $S_{B_i}$ , and by doublets distributed over the wake portion that is very close

to the trailing edge from which emanated (near wake,  $S_W^N$ ). The incident potential field is associated to doublets distributed over the complementary wake region that compose the far wake  $S_{W_f}$  [33].

In this formulation, the incident potential affects the scattered potential through the induced-velocity which modifies the boundary conditions of the scattered potential problem, while the scattered potential affects the incident potential by its trailing-edge discontinuity that is convected along the wake and gives the intensity of the vortices of the far wake. Exploiting the vortex-doublet equivalence, the incident velocity field is evaluated through the Biot-Savart law. In order to assure a regular distribution of the induced velocity field, and thus a stable and regular solution even when body-vortex impacts occur, a Rankine finite-thickness vortex model is used in the Biot-Savart law [33]. The shape of the wake surface is determined as part of the solution by moving the panel vertices with the velocity field induced by wakes and bodies.

Once the potential field is known, the Bernoulli theorem yields the pressure distribution [32] from which, in turn, aerodynamic loads can be readily evaluated.

### 2.3 Helicopter simulation tool

The *HELISTAB* code is a comprehensive helicopter code developed in the last decade at Roma Tre University. It considers rigid body dynamics, blade aeroelasticity, airframe elastic motion, as well as effects from actuators dynamics and stability augmentation systems. Passive and active pilot models are included, and both linear and non-linear analyses may be performed. *HELISTAB* has been validated and applied within the activities of the European Project ARISTOTEL, addressed to the study of Rotorcraft-Pilot Couplings phenomena [34;35;36;37].

The linearized equations of aeromechanics are written as a first order differential system,

$$(6) \quad \dot{z} = Az + Bu$$

where  $z$  collects Lagrangian coordinates of elastic blade and airframe deformations and their derivatives, airframe rigid-body (center-of-mass) linear and angular velocity components, Euler angles and inflow states,  $x$ , whereas  $u$  collects main and tail rotor controls and their first and second order derivatives, namely,  $u = \{\dot{\theta}_0, \theta_0, \theta_0, \dot{\theta}_s, \dots, \theta_p\}^T$ .

In the following, details concerning the derivation of matrices  $A$  and  $B$  in Eq. (6) are provided for aeromechanics formulations using both kinematic-based and loads-based dynamic inflow models.

### 2.4 Kinematic-based inflow

Recasting the vector of state variables as  $z = \{y \ x\}^T$ , coupling the rotor and airframe dynamics equations with the dynamic inflow model of Eq. (3) yields the following aerome-

chanics model

$$(7) \quad \begin{aligned} \dot{y} &= A_y y + C_\lambda \lambda + B_y u \\ \lambda &= A_{1y}^{wi} \dot{y} + A_{0y}^{wi} y + C^{wi} x + A_{0u}^{wi} u \\ \dot{x} &= B_y^{wi} y + A^{wi} x + B_u^{wi} u \end{aligned}$$

with  $C_\lambda$  collecting the derivatives of the aerodynamic generalized forces of the aeromechanics model with respect to  $\lambda$ . In addition, the matrices of the wake inflow model in Eq. (7) are obtained by re-organizing those in Eq. (3), to be consistent with the vectors of variables of the aeromechanics model (for instance, hub linear velocities considered in Eq. (3) are given as a combination of the airframe dofs considered in the vector  $y$ ).

Then, substituting the inflow model in the rotor/airframe dynamics equations, the following set of first-order differential equations governing the helicopter dynamics are obtained

$$(8) \quad \begin{aligned} \dot{y} &= (I - C_\lambda A_{1y}^{wi})^{-1} [(A_y + C_\lambda A_{0y}^{wi}) y + \\ &+ C_\lambda C^{wi} x + (B_y + C_\lambda A_{0u}^{wi}) u] \\ \dot{x} &= B_y^{wi} y + A^{wi} x + B_u^{wi} u \end{aligned}$$

from which matrices  $A$  and  $B$  of Eq. (6) may be easily identified.

### 2.5 Load-based inflow

When load-based inflow model is used, the aeromechanics equations may be written as

$$(9) \quad \begin{aligned} \dot{y} &= A_y y + C_\lambda \lambda + B_y u \\ \lambda &= C^{wi} x \\ \dot{x} &= A^{wi} x + B_f^{wi} f \end{aligned}$$

where the perturbative hub loads appearing in Eq. (9) are given by the following linearized form

$$(10) \quad f = F_y y + F_\lambda \lambda + F_u u$$

Finally, combining Eqs. (9) and (10) yields the following set of first-order differential equations governing the helicopter dynamics

$$(11) \quad \begin{aligned} \dot{y} &= A_y y + C_\lambda C^{wi} x + B_y u \\ \dot{x} &= B_f^{wi} F_y y + (A^{wi} + B^{wi} F_\lambda C^{wi}) x + B_f^{wi} F_u u \end{aligned}$$

from which matrices  $A$  and  $B$  of Eq. (6) may be readily identified.

## 3 NUMERICAL RESULTS

### 3.1 Aerodynamics validation

Light's work<sup>[18]</sup> has been chosen as benchmark to validate the aerodynamics solver in ground effect, in terms of tip vortex geometry and thrust. In that experiment, an untwisted four-bladed rotor (whose main data are summarized in Tab. 1) in hovering condition above a circular surface having a diameter of 6.62 rotor radii.

Span	1.105	m
Root Cut Off	0.425	m
Chord	0.18	m
Solidity	0.207	-
Airfoil	NPL 9165	-
Angular Velocity	172.3	rad/s

Table 1: Light's Four-Bladed rotor characteristics,<sup>[18]</sup>.

Figures 1 and 2 show the numerical tip vortex reconstruction compared with the experimental results (obtained by shadowgraph) at two different heights, namely  $z = 0.84 R$ , having a disk loading of  $C_T/\sigma = 0.071$  and  $z = 0.52 R$  having  $C_T/\sigma = 0.090$ . The wake shape proposed by Landgrebe<sup>[38]</sup> for OGE rotors is also shown as a reference.

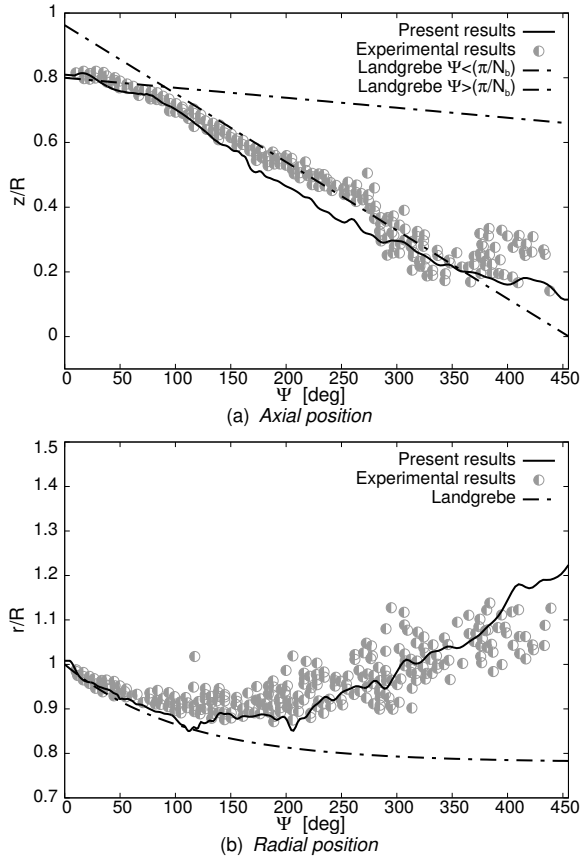


Figure 1: Comparison between Light's experiment,<sup>[18]</sup> BEM prediction and Landgrebe wake model in terms of axial and radial position of tip vortex for  $z = 0.84 R$  and  $C_T/\sigma = 0.071$ .

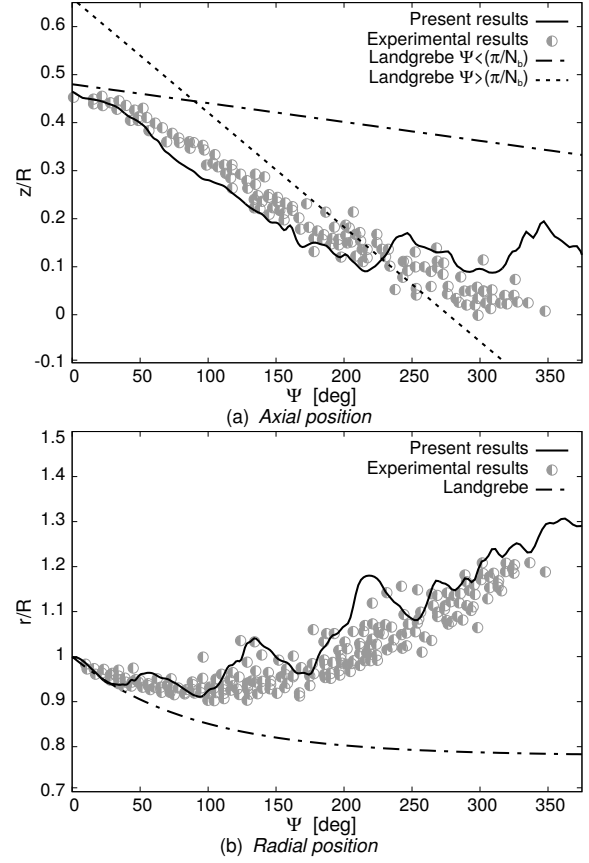


Figure 2: Comparison between Light's experiment,<sup>[18]</sup> BEM prediction and Landgrebe wake model in terms of axial and radial position of tip vortex for  $z = 0.52 R$  and  $C_T/\sigma = 0.090$ .

In both cases a good agreement between experimental results and numerical simulations is achieved, in particular in terms of wake distortion caused by the presence of the ground, clearly highlighted by the comparison with the Landgrebe wake shape which is a good approximation for Out-of-Ground-Effect hovering rotors. The capability of the present aerodynamic solver to well predict ground effect also on rotor loads is proved by Fig. 3. For a fixed collective pitch and different values of  $z/R$ , this figure shows the comparison in terms of the ratio of thrust in ground effect and out of ground effect between experimental results, three approximated analytical equations proposed in literature<sup>[39]</sup> and BEM numerical results.

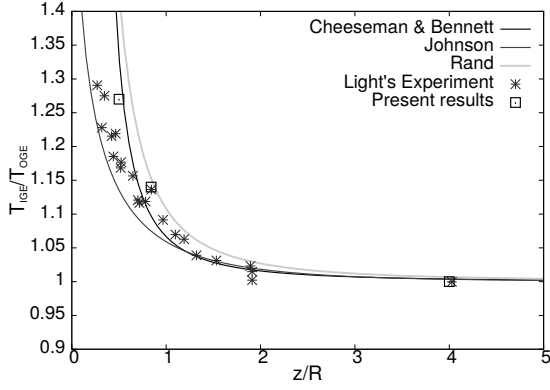


Figure 3: Ground effects on rotor thrust vs  $z/R$ .

### 3.2 Dynamic inflow model effect on aeromechanics

The test case examined is a mid-weight helicopter model inspired to the Bo-105, whose main data are reported in Sec. 3.2. Hovering flight at 1 diameter above the ground (simulated as a circle having twice the radius of the rotor) is examined, whereas the analysis in other steady conditions are left to future investigations. Moreover, only results obtained through the  $\lambda - f$  model obtained perturbing rotor controls are presented. The perturbations consist of chirp signals from 2 to 18 rad/s.

$mass$	2200	$kg$
$I_{xx}$	1430	$kg\,m^2$
$I_{yy}$	4975	$kg\,m^2$
$I_{zz}$	4100	$kg\,m^2$
$I_{xz}$	650	$kg\,m^2$
MR type	hingeless	-
MR radius	4.91	$m$
MR chord	0.27	$m$
MR angular speed	44.4	$rad/s$
MR blade twist	-8	$o/m$
MR number of blades	4	-
TR radius	1	$m$
TR chord	0.2	$m$
TR angular speed	230	$rad/s$
TR number of blades	2	-

Table 2: Main helicopter data

First, the effect of ground on inflow is analyzed in ?? and Fig. 5, which show OGE and IGE transfer functions along with the RMA approximation of IGE ones, in the range of frequency of interest for flight dynamics. The former relates axisymmetric variables ( $\lambda_0$  vs  $C_T$ ), while the latter antisymmetric ones ( $\lambda_c$  vs  $C_M$ ). Note that, due to the axial symmetry of the flight condition, the inflow transfer matrix is expected to be block diagonal, *i.e.* the thrust coefficient induces only  $\lambda_0$  and rolling and pitching moment coefficients

influence only  $\lambda_s$  and  $\lambda_c$ . Here, the off-axis transfer functions  $\lambda_s$  vs  $C_M$  and  $\lambda_c$  vs  $C_L$  are not shown, being significantly smaller than the on axis  $\lambda_s$  vs  $C_L$  and  $\lambda_c$  vs  $C_M$  (which are, in turn, equivalent). The effect of ground is opposite on axisymmetric and antisymmetric transfer functions. In particular, the magnitude of  $\lambda_0$  vs  $C_T$  is reduced by the presence of the ground, whereas that of  $\lambda_c$  vs  $C_M$  is increased. Moreover, the phase of the transfer function  $\lambda_c$  vs  $C_M$  is significantly affected by the ground, which causes an additional delay with the respect to OGE case, in the frequencies range above 0.1 Hz (see Fig. 5).

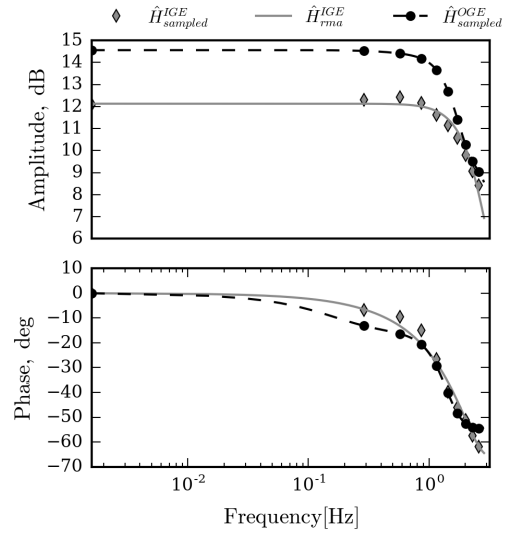


Figure 4:  $\lambda_0$  vs  $C_T$  transfer function.

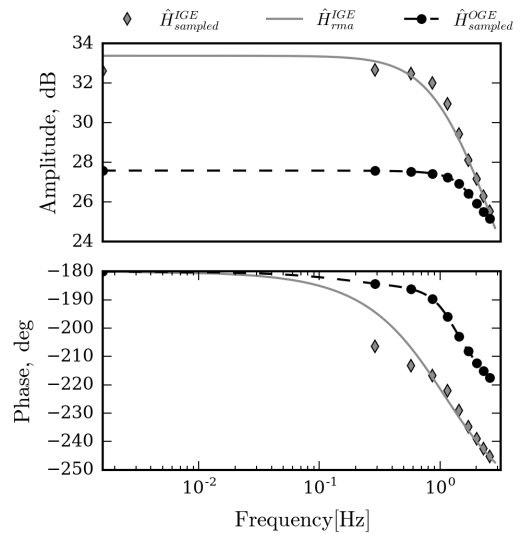


Figure 5:  $\lambda_c$  vs  $C_M$  transfer function.

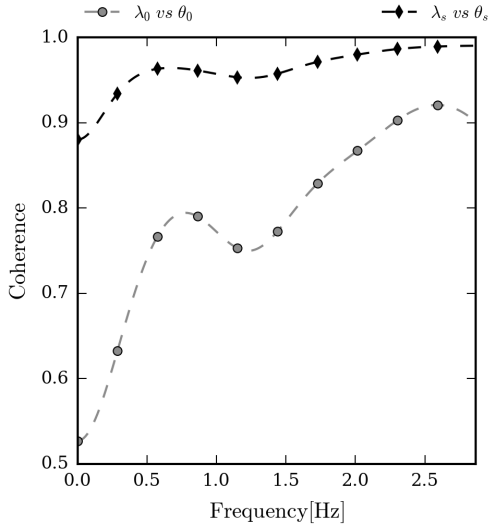


Figure 6: Coherence between inflow coefficients and kinematic degrees of freedom.

Figure 6 shows the coherence between input (kinematic degrees of freedom) and output (inflow coefficients) signals. While the coherence from antisymmetric variables (e.g.  $\lambda_s$  vs.  $\theta_s$ ) is very high (above 0.9 in the range of frequency characterizing the input chirp signal), that between  $\theta_0$  and  $\lambda_0$  is significantly smaller, although acceptable. Note that the amplitude of perturbation on  $\theta_0$  has been increased from 1 deg (used in this work for antisymmetric perturbations) to 3 deg, since for lower values the resulting coherence was even lower. This is probably due to numerical round-off and truncation errors. However, to clarify this aspect future additional investigations are required.

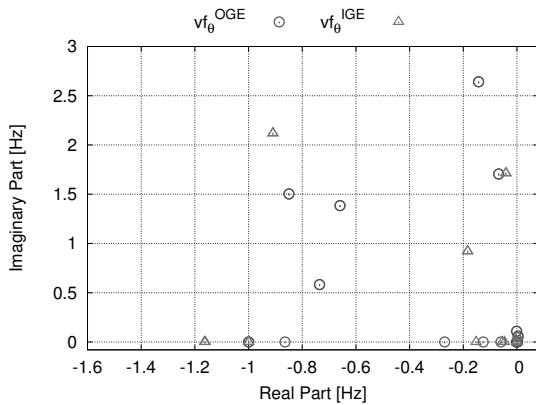


Figure 7: Effect of the presence of the ground on root locus.

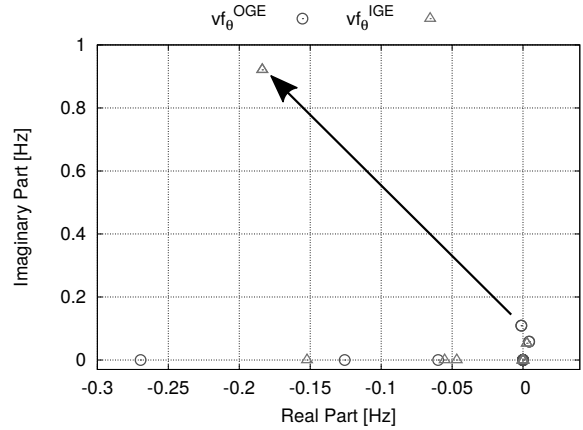


Figure 8: Effect of the presence of the ground on root locus, detail.

Figures 7 and 8 highlight the effect of the ground presence on the helicopter dynamic stability. The most relevant effect is the shift of the dutch roll poles complex pair, which increases his damping and natural frequency, as highlighted in Fig. 8. This fact has a significant impact on aeromechanic transfer functions, shown in Figs. 9 to 13. The former four report on axis transfer function, while the latter is related to cross-coupling dynamics.

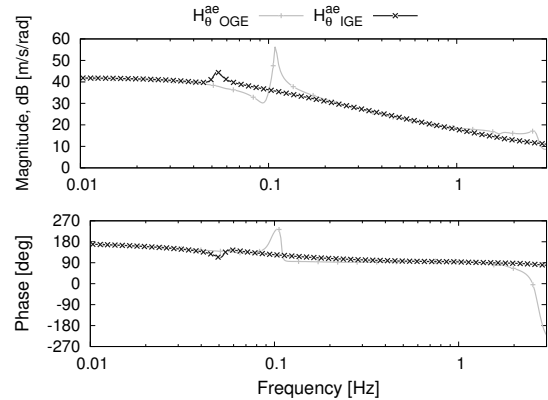


Figure 9:  $w$  vs  $\theta_0$  transfer function in and out of ground effect.

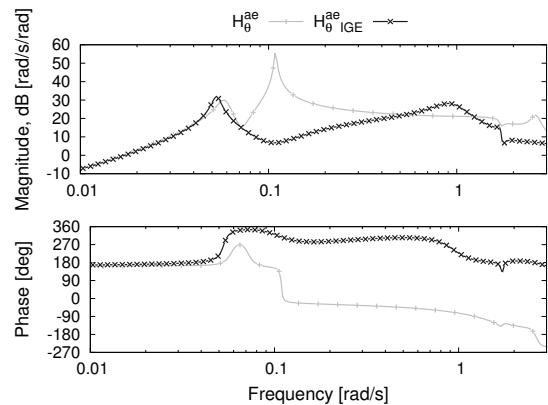


Figure 10:  $q$  vs  $\theta_s$  transfer function in and out of ground effect.

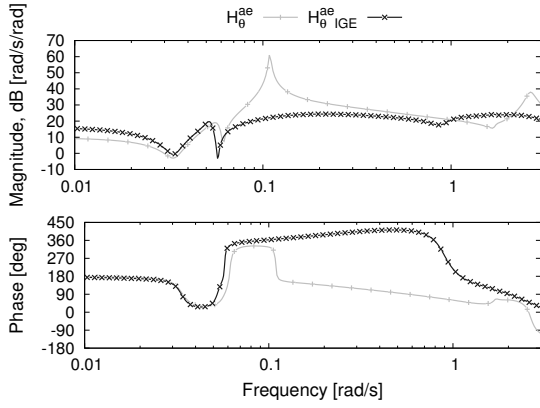


Figure 11:  $p$  vs  $\theta_c$  transfer function in and out of ground effect.

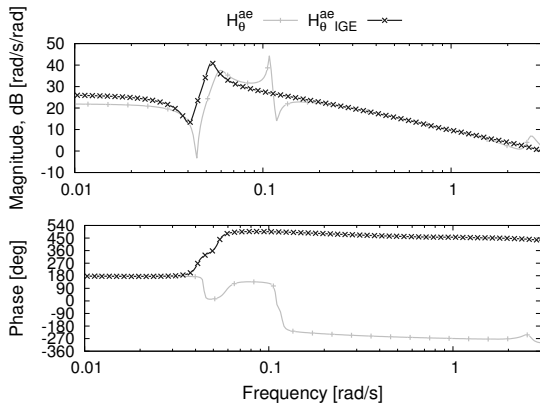


Figure 12:  $r$  vs  $\theta_p$  transfer function in and out of ground effect.

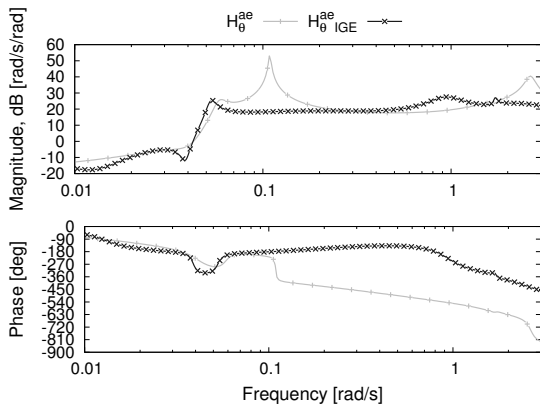


Figure 13:  $p$  vs  $\theta_s$  transfer function in and out of ground effect.

Indeed, coherently with the shift of dutch roll mode, the helicopter response is significantly modified at about 0.1 Hz. In particular, the peak of the response associated to that pole, which is particularly pronounced out of ground effect especially in the transfer functions related to cyclic controls, disappears from the Bode plot. Moreover, the steady response is slightly affected by the presence of the ground, only as regards roll and yaw responses.

## 4 CONCLUSIONS

Two different approaches to dynamic inflow modeling of rotor in ground effect conditions have been presented. In the first, inflow coefficients are related to the kinematic degrees of freedom, while the second one considers the relation between inflow coefficients and rotor loads (as in the well known Pitt-Peters' model). The identification of the inflow transfer matrix is based on time marching Boundary Element Method simulation of the rotor in presence of the ground and is followed by a Rational Matrix Approximation, in order to obtain a state-space inflow model.

The aerodynamic solver has been validated against experiments from the literature, showing a good accuracy in the prediction of both aerodynamic loads and wake shape. Its application to the identification of the dynamic inflow model in ground effect has been more difficult with respect to that in out-of-ground-effect case. In particular, the identification process of the transfer functions involving axisymmetric components of the inflow has been significantly more difficult, requiring an appropriate regularization of numerical free-wake algorithm to take into account the presence of the ground. Finally, from the preliminary aeromechanic analysis performed in this paper, the most relevant effect of the ground presence has been noticed in the shift of the dutch roll poles, which primarily affect roll response to cyclic controls.

## 5 ACKNOWLEDGEMENTS

This research was performed within the Roma Tre University participation in the University of Maryland/U.S.Naval Academy Vertical Lift Research Center of Excellence.

## References

- [1] G. Morrison, *Helicopter safety offshore*. HSE Books, 2001.
- [2] J. Smith and W. Mitchell, "Aircraft/ship interface problems - the u.s. navy's program," in *AIAA/SNAME Advanced Marine Vehicles Conference*, no. AIAA-PAPER 74-305, February 1974.
- [3] R. M. Tuttle, "A study of helicopter landing behavior on small ships," *Journal of the American Helicopter Society*, vol. 21, no. 2, pp. 2–11, 1976.
- [4] C. Kääriä, Y. Wang, J. Curran, J. Forrest, and I. Owen, "Aerodyn: An airwake dynamometer for measuring the impact of ship geometry on helicopter operations," in *36th European Rotorcraft Forum, Paris*, pp. 7–9, 2010.
- [5] C. H. Kääriä, Y. Wang, G. D. Padfield, J. S. Forrest, and I. Owen, "Aerodynamic loading characteristics of a model-scale helicopter in a ship's airwake," *Journal of Aircraft*, vol. 49, no. 5, pp. 1271–1278, 2012.

- [6] S. J. Hodge, J. S. Forrest, G. D. Padfield, and I. Owen, "Simulating the environment at the helicopter-ship dynamic interface: research, development and application," *Aeronautical Journal*, vol. 116, no. 1185, p. 1155, 2012.
- [7] S.-R. Oh, K. Pathak, S. K. Agrawal, H. R. Pota, and M. Garrett, "Autonomous helicopter landing on a moving platform using a tether," in *Proceedings of the 2005 IEEE International Conference on Robotics and Automation*, pp. 3960–3965, IEEE, 2005.
- [8] J. A. Lusardi, M. B. Tischler, C. L. Blanken, and S. J. Labows, "Empirically derived helicopter response model and control system requirements for flight in turbulence," *Journal of the American Helicopter Society*, vol. 49, no. 3, pp. 340–349, 2004.
- [9] G. H. Gaonkar, "Review of turbulence modeling and related applications to some problems of helicopter flight dynamics," *Journal of the American Helicopter Society*, vol. 53, no. 1, pp. 87–107, 2008.
- [10] K. A. Schau, "Developing interpretive turbulence models from a database with applications to wind farms and shipboard operations," msc thesis, Florida Atlantic University, 2013.
- [11] K. Schau, G. Gaonkar, and S. Polsky, "Rotorcraft downwash impact on ship airwake: statistics, modelling, and simulation," *The Aeronautical Journal*, vol. 120, no. 1229, pp. 1025–1048, 2016.
- [12] W. Wiesner and G. Kohler, "Tail rotor performance in presence of main rotor, ground, and winds," *Journal of the American Helicopter Society*, vol. 19, no. 3, pp. 2–9, 1974.
- [13] W. T. Yeager Jr, W. H. Young Jr, and W. R. Mantay, "A wind-tunnel investigation of parameters affecting helicopter directional control at low speeds in ground effect," Tech. Rep. TN D-7694, NASA, 1974.
- [14] R. Empey and R. Ormiston, "Tail-rotor thrust on a 5.5-foot helicopter model in ground effect," in *American Helicopter Society Annual National Forum, Washington, DC*, 1974.
- [15] H. Curtiss, M. Sun, W. Putman, and E. Hanker, "Rotor aerodynamics in ground effect at low advance ratios," *Journal of the American Helicopter Society*, vol. 29, no. 1, pp. 48–55, 1984.
- [16] E. J. Hanker and R. P. Smith, "Parameters affecting helicopter interactional aerodynamics in ground effect," *Journal of the American Helicopter Society*, vol. 30, no. 1, pp. 52–61, 1985.
- [17] J. CIMBALA, M. BILLET, D. GAUBLomme, and J. OEFELEIN, "Experiments on the unsteadiness associated with a ground vortex," *Journal of Aircraft*, vol. 28, no. 4, pp. 261–267, 1991.
- [18] J. S. Light, "Tip vortex geometry of a hovering helicopter rotor in ground effect," *Journal of the American Helicopter Society*, vol. 38, no. 2, pp. 34–42, 1993.
- [19] J. Kucab, M. Moulton, M. Fan, and J. Steinhoff, "The prediction of rotor flows in ground-effect with a new hybrid method," in *17th Applied Aerodynamics Conference*, no. 99-3222, (Norfolk, VA), p. 3222, June 1999.
- [20] N. Kang and M. Sun, "Simulated flowfields in near-ground operation of single- and twin-rotor configurations," *Journal of Aircraft*, vol. 37, pp. 214–220, Mar 2000.
- [21] H. Xin, J. Prasad, D. Peters, T. Nagashima, and N. Iboshi, "A finite state inflow model for simulation of helicopter hovering in ground effect," in *ANNUAL FORUM PROCEEDINGS-AMERICAN HELICOPTER SOCIETY*, vol. 54, pp. 777–784, AMERICAN HELICOPTER SOCIETY, 1998.
- [22] H. Xin, J. V. R. Prasad, and D. A. Peters, "Inflow model for simulation of helicopter flight in dynamic ground effect," in *25th European Rotorcraft Forum, Rome, IT*, 1999.
- [23] H. Xin, J. Prasad, and D. Peters, "Dynamic inflow modeling for simulation of a helicopter operating in ground effect," in *Modeling and Simulation Technologies Conference and Exhibit*, p. 4114, 1999.
- [24] M. Gennaretti, C. Pasquali, F. Cardito, J. Serafini, G. Bernardini, and R. Celi, "Dynamic wake inflow modeling in ground effect for flight dynamics applications," in *AHS 73rd Annual Forum & Technology Display*, (Fort Worth, TX), June 2017.
- [25] M. Gennaretti, R. Gori, J. Serafini, G. Bernardini, and F. Cardito, "Rotor dynamic wake inflow finite-state modelling," in *Proceedings of the 33rd AIAA Applied Aerodynamics Conference*, Dallas, TX, 2015.
- [26] M. Gennaretti, R. Gori, F. Cardito, J. Serafini, and G. Bernardini, "A space-time accurate finite-state inflow model for aeroelastic applications," in *Proceedings of the 72nd Annual Forum of the American Helicopter Society*, West Palm Beach, Florida, 2016.
- [27] M. Gennaretti, R. Gori, J. Serafini, F. Cardito, and G. Bernardini, "Identification of rotor wake inflow finite-state models for flight dynamics simulations," *CEAS Aeronautical Journal*, vol. 8, no. 1, pp. 209–230, 2017.
- [28] J. Serafini, F. Cardito, G. Bernardini, and M. Gennaretti, "Application of low-order wake inflow models to rotorcraft aeromechanics," in *International Forum on Aeroelasticity and Structural Dynamics*, (Como, Italy), June 2017.
- [29] D. M. Pitt and D. A. Peters, "Theoretical Predictions of Dynamic Inflow Derivatives," *Vertica*, vol. 5, pp. 21–34, 1981.
- [30] D. M. Pitt and D. A. Peters, "Rotor dynamic inflow derivatives and time constants from various inflow models," in *15th European Rotorcraft Forum: September 13-15, 1983, Stresa, Italy*, 1983.
- [31] R. Gori, J. Serafini, M. Molica Colella, and M. Gennaretti, "Assessment of a state-space aeroelastic rotor model for rotorcraft flight dynamics," *CEAS Aeronautical Journal*, vol. 7, no. 3, pp. 405–418, 2016.
- [32] G. Bernardini, J. Serafini, M. Molica Colella, and M. Gennaretti, "Analysis of a structural-aerodynamic fully-coupled formulation for aeroelastic response of rotorcraft," *Aerospace Science and Technology*, vol. 29, no. 1, pp. 175–184, 2013.
- [33] M. Gennaretti and G. Bernardini, "Novel boundary integral formulation for blade-vortex interaction aerodynamics of helicopter rotors," *AIAA Journal*, vol. 45, no. 6, pp. 1169–1176, 2007.

- [34] M. Gennaretti, J. Serafini, P. Masarati, and G. Quaranta, "Effects of Biodynamic Feedthrough in Rotorcraft/Pilot Coupling: Collective Bounce Case," *Journal of Guidance, Control, and Dynamics*, vol. 36, no. 6, pp. 1709–1721, 2013.
- [35] M. D. Pavel, M. Jump, B. Dang-Vu, P. Masarati, M. Gennaretti, A. Ionita, L. Zaichik, H. Smaili, G. Quaranta, D. Yilmaz, *et al.*, "Adverse rotorcraft pilot couplings—past, present and future challenges," *Progress in Aerospace Sciences*, vol. 62, pp. 1–51, 2013.
- [36] M. D. Pavel, P. Masarati, M. Gennaretti, M. Jump, L. Zaichik, B. Dang-Vu, L. Lu, D. Yilmaz, G. Quaranta, A. Ionita, and Others, "Practices to identify and preclude adverse Aircraft-and-Rotorcraft-Pilot Couplings—A design perspective," *Progress in Aerospace Sciences*, vol. 76, pp. 55–89, 2015.
- [37] J. Serafini, M. Molica Colella, and M. Gennaretti, "A finite-state aeroelastic model for rotorcraft–pilot coupling analysis," *CEAS Aeronautical Journal*, vol. 5, no. 1, pp. 1–11, 2014.
- [38] A. J. Landgrebe, "An analytical model for predicting rotor wake geometry," *Journal of American Helicopter Society*, vol. 14, no. 4, pp. 20–32, 1969.
- [39] V. Khromov and O. Rand, "Ground effect modeling for rotary-wing simulation," in *ICAS 2008- International Congress of The Aeronautical Sciences*, 2008.